JOURNAL OF MATERIALS SCIENCE 27 (1992) 6229–6240

# Effect of water absorption on residual stresses in injection-moulded nylon 6,6

M. W. A. PATERSON*, J. R. WHITE
*Materials Division, Department of Mechanical, Materials and Manufacturing Engineering, University of Newcastle upon Tyne, Newcastle upon Tyne NE1 7RU, UK*

The layer removal procedure has been used to examine the effect of water on residual stresses in injection-moulded nylon 6,6. Nylons are highly sensitive to moisture and a method based on a Karl–Fischer titration was used to measure distribution of water within the mouldings. In the dry state or with a modest water content the moulding possessed surface compressive stresses and tensile stresses in the interior. Large amounts of water absorption caused a reversal of the stress sense due to secondary crystallization causing a relative volume change between the skin and core. Two other influences of water have been identified: (i) preferential swelling introduced additional strains; and (ii) water-induced plasticization which lowers the modulus, thus changing the stress distribution. Simple models to predict the changes in the residual stress distribution have been developed and the results agree with experimental measurements.

## 1. Introduction

Many engineering and commodity products are made from nylon materials by injection moulding. Most nylons absorb water readily and as a consequence their properties are modified significantly [1–3]. Another characteristic of injection mouldings that can influence properties is the residual stress distribution, and the purpose of the study described here was to investigate the interaction between water absorption and residual stress distribution, choosing as the model material a commercial grade nylon 6,6.

In nylon 6,6, both liquid water and water vapour can be absorbed from the surroundings in a proportion approaching 9% by weight [1]. The absorbed water penetrates only the amorphous phase [4, 5] and its presence has a plasticizing effect that facilitates molecular chain movement [6–8]; this decreases stiffness but increases flexibility [2]. Changes occur in the glass transition temperature, $T_g$, electrical properties [9] and mechanical properties [10] as a function of moisture content, in both oriented and unoriented nylons [5]. Even a few tenths of a per cent of water cause the modulus to fall significantly from the value in dry nylon at room temperature. However, moisture is not always detrimental to properties and nylon which has been equilibrated with atmospheric humidity has improved toughness, elongation to break and impact resistance compared with the dry material. More detailed accounts of the effects of moisture on mechanical properties can be found in References 1 and 2. In general, increasing the water content has a similar effect to an increase in temperature or the time-scale of the test [10]. The quantity of water in any given nylon sample depends on the physical structure, the temperature during absorption and the time allowed for absorption, the conditions of absorption (i.e. immersion in liquid or the relative humidity if in vapour) and sample thickness. If water is distributed in a non-uniform manner this will cause property variations to develop within the moulding. This is often ignored, and an examination of the importance of this effect is included in the study presented here.

Under normal cooling conditions a moulded article usually develops a quasi-parabolic stress distribution, with compressive stresses in the surface regions and weaker tensile stresses in the interior [3, 11, 12]. The formation of residual stresses is often unavoidable and it is difficult to control the magnitude of the stresses, especially when moulding complicated shapes. When freshly moulded and before exposure to water, injection-moulded nylons contain residual stresses that are compressive near the surface and tensile in the interior [3, 12]. The absorption of water has a plasticizing effect that may permit relaxations that do not occur in the dry state, or may accelerate relaxations that occur slowly in the absence of water, so modifying the residual stress distribution and its ageing characteristics. At water saturation the stress distribution has been found to be reversed with tensile stresses near the surface and compressive stresses in the interior [3, 12]. Russell and Beaumont [12] attributed this stress reversal to secondary crystallization caused by the uptake of water. This is not the only water-promoted cause of change in the residual stresses, for water absorption also induces swelling and reduces the modulus. This paper is primarily concerned with residual stresses and the effect of water absorption on these stresses.

---

* *Present address*: Courtaulds Coatings, Felling, Gateshead, Tyne and Wear, UK.

## 2. Experimental procedure

### 2.1. Materials and conditions

The test samples were moulded on a Butler–Smith 100/60 reciprocating screw machine in the form of standard end-gated straight bars, having the approximate dimensions: length, 190 mm, width, 12.7 mm and thickness, 3.2 mm. The nylon 6,6 material used to prepare the samples was ICI Maranyl A100S. Before moulding, the material was thoroughly dried in a vacuum oven for at least 4 h at 90 °C. Moulding conditions were chosen according to the manufacturer's technical literature [13] as shown in Table I, and these produced void-free, visually acceptable mouldings. The mould temperature was controlled by a Churchill Junior SW140 water circulating temperature controller.

The mouldings were placed in bags containing silica gel immediately after ejection to prevent water absorption. For prolonged dry storage the batches of samples were placed in a vacuum until required. To check that no water absorption occurred from vacuum storage, batches were weighed before and after storing. The bars showed no weight gain.

### 2.2. Specimen conditioning

In this investigation three types of nylon 6,6 samples were studied: (i) bars stored in the dry state as described above and termed "dry" bars; (ii) bars allowed to equilibrate with atmospheric moisture and called "conditioned" bars; and (iii) water "saturated" bars which were stored for a prolonged period immersed in water at room temperature and removed just prior to testing. The dry bars contained a negligible amount of water and the wet bars contained about 9% by weight of water, having been stored in water long enough to reach saturation.

### 2.3. Specimen preparation

Thin test samples were produced from selected locations within the bars by milling away the material to a chosen depth on either side. Each moulding was fixed to the milling block and a single blade cutter passed over the sample using a fly cutting action to remove a depth of up to 0.3 mm in a single sweep. The best surface finishes for nylon 6,6 were obtained with a cutter advance speed of 25.4 mm min$^{-1}$ and a cutter rotation speed of 2240 r.p.m.

The milling procedure has been used extensively in this laboratory [11, 14] and the milling parameters chosen were based on this experience. As in earlier cases, no excessive surface heating was apparent and it is unlikely that the machining operation caused the sample to change its state through relaxation processes or secondary crystallization.

### 2.4. Measurements of water concentration

A simple and direct method of determining moisture levels is to measure weight gain on exposure to water [7, 8, 15]. This method cannot indicate whether or not the distribution of water within the moulding is uniform. The most common technique for measuring moisture levels in nylons is based on the Karl–Fischer titration [2] (ASTM D789) and by extracting samples from different locations within the moulding this method can be used to determine variations in moisture content. The method is based on a titration reaction between iodine, sulphur dioxide and water in aqueous solution and can be represented as

$$I_2 + SO_2 + 2H_2O = 2HI + H_2SO_4$$

The water is removed from a sample by heating it to 255 °C and passing dry nitrogen gas over it. The gas picks up the water and is bubbled through moisture-free methanol into which the moisture is transferred. This is then titrated with Karl–Fischer reagent to determine the mass of water driven off. Knowing the mass of the sample it is possible to determine the fractional water content present [3]. Samples were extracted from different depths within moulded bars conditioned in various ways using the milling procedure described above.

### 2.5. Dynamic mechanical thermal analysis

Dynamic mechanical analysis was conducted on samples of nylon 6,6 both in the dry state and after water conditioning. These measurements had two aims: first, to show the effect of water on dynamic mechanical properties; and second, to determine the Young's modulus variations through the depth of a sample.

The nylon 6,6 samples were scanned over a temperature range − 100–200 °C at a heating rate of 4 °C min$^{-1}$ using a Polymer Laboratories Dynamic Mechanical Thermal Analyzer (DMTA). A frequency of 1 Hz was used for all the runs reported here.

When testing bars taken from dry storage the following procedure was adopted. On removing a bar from the vacuum it was cut into two halves, one of which was used to prepare several samples by the milling procedure. These were tested on the DMTA as quickly as possible to minimize water absorption, giving results for "dry" bars. The second half of the bar was stored in laboratory air for 6 months before preparation and testing. This allowed water absorption to occur producing "conditioned" bars. The test

TABLE I Moulding conditions for nylon 6,6

| Polymer | Temperature (°C) | | | | Injection pressure (MPa) | Injection time time (s) | Cooling time time (s) |
|---|---|---|---|---|---|---|---|
| | Zone 1 | Zone 2 | Nozzle | Mould | | | |
| ICI maranyl A100S nylon 6,6 | 250 | 285 | 220 | 90 | 150 | 10 | 20 |

samples, about 0.2 mm thick, were extracted from different depths of each bar enabling a study of through-thickness variations in dynamic mechanical properties. In this way each bar was used to make two samples from the same depth location, one in the dry state and the other conditioned. Comparisons were then free from any variations between different bars. For nylon 6,6 bars which were water-saturated by storage in water, test samples were prepared from the surface, the core, and an intermediate depth, and tested on the DMTA.

The standard Polymer Laboratories DMTA bending test head was used. The samples were mounted in single cantilever bending; this arrangement allows the drive shaft a certain amount of lateral movement and can thus accommodate dimensional changes when the temperature changes more easily than the dual cantilever mode. The pressure with which the clamp bars are tightened is very important as over-tightening causes compression of the sample. To ensure consistent clamping the following procedure was used. The clamps were tightened lightly and the dynamic mechanical measurement was made at room temperature. Then the driving mechanism was switched off, the clamps were tightened a little more and the measurement repeated; an increase in the indicated modulus was normally observed. This procedure was repeated and the clamps were tightened progressively until no increase in the indicated modulus values occurred, i.e. a plateau region was reached. The use of a torque screwdriver enabled reproducible clamping pressures to be used. Clamping irregularities are thought to be the major source of errors and as a further check for correct clamping, an oscilloscope was used to monitor the sample vibration using a signal derived from the DMTA displacement transducer. Any irregularities in the sine waves indicated incorrect clamping and the run was abandoned. The data are presented in the form of the logarithm of the storage Young's modulus, log $E'$, and the loss tangent, tan $\delta$, against temperature.

The absolute accuracy of the modulus values obtained with the DMTA machine must be regarded with some caution. On comparing the modulus values with the results obtained by static bending tests it is apparent that the DMTA results are significantly lower. The accuracy of the results is highly dependent on the geometry constant and clamping arrangement. The main error in calculating the geometry constant (a calibration constant derived from the cross-section moment of inertia of the sample and the clamping arrangement used) is in estimating the effective length of the sample being deformed. This is not simply the length between the clamp faces as there is some movement of the sample underneath the clamps. This end effect is the same for all sample lengths so that the most accurate modulus results are obtained with the largest sample length available. In this study thin samples were required to enable through-depth variations in properties to be investigated and this demanded the use of short specimens in order to maintain the geometry constant within the bounds recommended by the manufacturer for optimal operation. It is possible to improve the accuracy of the modulus values by plotting 1/(indicated modulus)$^{1/3}$ versus length, $l$; this should give a straight line, the gradient of which is used to give the true modulus, but this was not attempted here because the range of lengths available, as restricted by the other constraints, was too small.

### 2.6. Determination of through-depth modulus profiles

Modulus variations within an injection moulding occur as a result of thermal and shear stresses that develop during moulding [16–19]. Subsequent to moulding, the plasticizing effect of any water absorbed also has a large effect on the magnitude and distribution of Young's modulus. To determine the Young's modulus distribution a bend test and layer removal technique were developed [20] and used for nylon 6,6 injection mouldings containing different amounts of water.

#### 2.6.1. Theory

The method of measurement involves conducting a three-point-bend test on a bar and then removing a layer of thickness, $a$, from each surface. The bar is then re-tested in three-point-bending. This cycle of removing layers and testing is repeated until the sample is too thin to continue. The minimum thickness for satisfactory testing is about 0.7 mm with this material. The total span between the two outer supports in the three-point-bend test was 74 mm for the tests with bar thicknesses 1.7–3.2 mm, and 41 mm for smaller thicknesses in the latter stages of a set of measurements.

The bend tests all gave a linear relationship between the force, $F$, and deflection, $\delta$, and it can be assumed that errors in the bending analysis caused by shear deflections and friction at the supports can be neglected. The gradient, $F/\delta$, was recorded for each bar thickness tested and from this was calculated the quantity $S(a)$

$$S(a) = \frac{Fl^3}{6\delta} \tag{1}$$

$S(a)$ is plotted versus $a$ and the gradient, $\mathrm{d}S(a)/\mathrm{d}a$ is measured at intervals along the smooth curve. Next these gradients are substituted into the following equation

$$E(z) = -\frac{\mathrm{d}S(a)}{\mathrm{d}a}\left(\frac{1}{2b(z_0 - a)^2}\right) \tag{2}$$

where $E(z_0 - a)$ is Young's modulus at $a$ from the bar surface, $b$ is the bar width and $2z_0$ is the original thickness of the bar. Throughout the above analysis it is assumed that the modulus distribution is symmetrical about the neutral plane. This should be the case for injection-moulded bars cooled equally from both sides. With the bars studied here it was found that after removal of equally thick layers from both surfaces no bending occurred, indicating that both the residual stress distribution and Young's modulus were probably symmetrical. The main limitation to this procedure is that the modulus distribution cannot be found within the central part of the bar for which satisfactory bend tests cannot be performed.

## 2.7. Residual stress analysis

Residual stresses develop as a result of inhomogeneous cooling during processing [11]. In injection moulding a temperature gradient is set up during cooling. The surface material solidifies very rapidly, then solidification takes place progressively inwards. This has the effect of producing high compressive stresses in the skin and weaker tensile stresses in the interior [3, 11, 12]. The method used in this laboratory to measure residual stresses in polymer bars is based on a layer removal procedure devised by Treuting and Read [21].

The following assumptions are made when using the Treuting and Read procedure:

(i) The stress should not vary in the plane of the specimen.
(ii) The removal of each surface layer should not disturb the stress distribution in the remaining material.
(iii) The elastic constants should be constant throughout the material and the sample should be linear in pure bending, i.e. the specimen bends to form an arc of a circle.

It is realised that Young's modulus is not constant throughout the depth but earlier work by Paterson and White [22], who developed a modified approach, demonstrated that the effect of modulus variations through thickness causes no serious errors in the residual stress distributions of nylon 6,6 samples obtained using the unmodified analysis. The unmodified analysis of Treuting and Read has been used in the studies reported below because it is much simpler and quicker to perform than the method of Paterson and White. It has been assumed that the Poisson's ratio, ν, is not depth dependent; accurate values of Poisson's ratio are rarely known for polymer mouldings and in any case the analysis is not very sensitive to variations in Poisson's ratio within the range of values commonly found for thermoplastics.

### 2.7.1. *Experimental procedure*

The method of layer removal by milling using a single point cutter with fly cutting action, and the use of the optical lever principle for curvature measurements has been described before [14]. The milling process was improved by using a vacuum clamping device to hold the sample in place during the cutting operation. In previous studies double-sided adhesive tape was used to secure the sample to the machining bed. This required very careful removal of the sample at the end of each milling operation to avoid overstressing; the use of the vacuum device circumvented this problem and speeded up the process. The new device consists of a rectangular block drilled with small holes that lead into a central bore hole that is connected to a vacuum pump. To ensure a good seal a thin strip of rubber with cut-outs matching the vacuum ports was placed between the sample and the milling block.

The analysis used here is based on a simplified version of the Treuting and Read [21] biaxial equation suitable when the bar curves significantly in one direction only. Measurements of curvature, $\rho_y$, in the width direction are difficult to make, but visual observation showed that it was fairly small. As long as $\rho_y < \rho_x$ the error incurred by taking it to be zero is not serious [11], and this leads to the expression given below in Equation 3. Plots of curvature versus depth of material removed, $(z_0 - z_1)$, were used to obtain the data required to substitute into this expression

$$\sigma_{i,x}(z_1) = \frac{-E}{6(1-\nu^2)}\left[(z_0 + z_1)^2\frac{d\rho_x(z_1)}{dz_1} + 4(z_0 + z_1)\rho_x(z_1) - 2\int_{z_1}^{z_0}\rho_x(z)dz\right] \tag{3}$$

where $\sigma_{i,x}(z_1)$ is the residual stress in the $x$-direction at the plane $z_1$ from the mid-plane of the specimen prior to layer removals, $\rho_x$ is the curvature in the $x$-direction, $E$ is Young's modulus and $\nu$ is Poisson's ratio.

## 3. Results and discussion

### 3.1. Water concentration

#### 3.1.1. *Conditioning in laboratory air*

The overall weight gain for samples of nylon 6,6 conditioned for 6 months in laboratory air was 1.9–2.0%. Fig. 1 shows the results of the Karl–Fischer procedure applied to samples extracted from different depths. This shows that the maximum concentration ( > 2%) is present near the surface, falling to lower values in the interior. This correlates quite well with theoretical predictions based on Fick's law, though an exact theoretical analysis is difficult to perform since

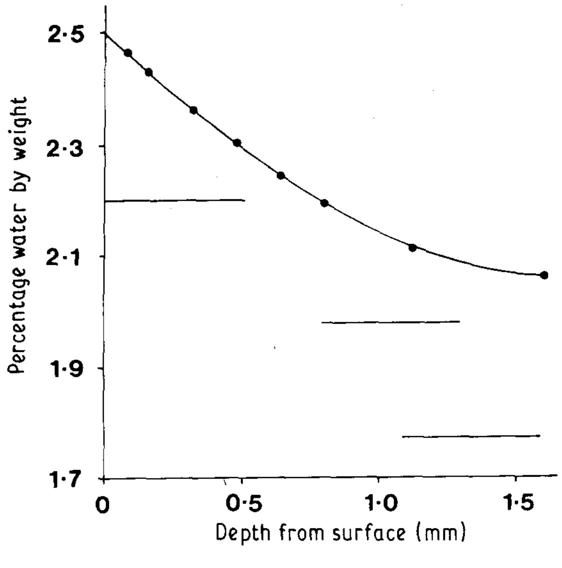

*Figure 1* Water concentration profile for a nylon 6,6 bar stored in laboratory air for 6 months ("conditioned"). The horizontal lines represent the experimental measurements and the curve is calculated using Fick's law.

the diffusion coefficient is a function of both crystallinity and water content, which both vary with position and time.

### *3.1.2. Conditioning immersed in water*

The water concentration profile for a nylon 6,6 bar after total immersion in water for 6 months is shown in Fig. 2. This time the variation in values measured at different depths is small, all values being close to 8% by weight. The overall weight change indicated absorption of about 9% by weight. The linear dimensions of the bars immersed in water was considerably higher than those of the dry bars, with the length increasing by 2.4%, the width by 3.2% and the thickness by 2.7%. This gives an overall value change of about 8.5%, showing that the water tends to cause swelling rather than occupying pre-existing space between the molecules. It has been estimated by others [4] that the volumetric change is actually approximately 80% of the volume of the water taken up. The water is believed to penetrate only the amorphous regions [5, 9] and disrupts the hydrogen bonding [9, 23].

### 3.2. Dynamic mechanical thermal analysis

Fig. 3 shows examples of DMTA scans of samples extracted from selected regions through the depth of bars made from unfilled nylon 6,6. Results are given for pairs of samples taken from the same bar, one in the dry state and the other after conditioning in air for 6 months as described above. Note that the conditioned specimens were machined from the half bar just before the DMTA test and should contain the equilibrium water content for the depth sampled. Two relaxation peaks are observed in the temperature range − 100 °C to 200 °C. The α-relaxation peak is found at about 75 °C in the dry state and is the glass transition region. The β-relaxation occurs at about − 60 °C and is believed to correspond to motion of the free amide

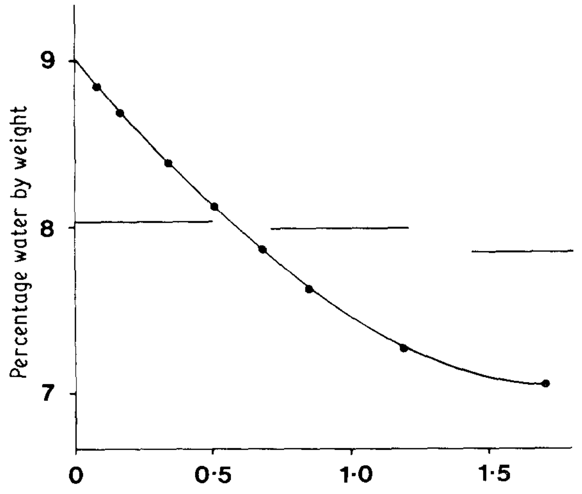

*Figure 2* Water concentration profile for a nylon 6,6 bar after immersion in water for 6 months ("saturated"). The horizontal lines represent the experimental measurements and the curve is calculated using Fick's law.

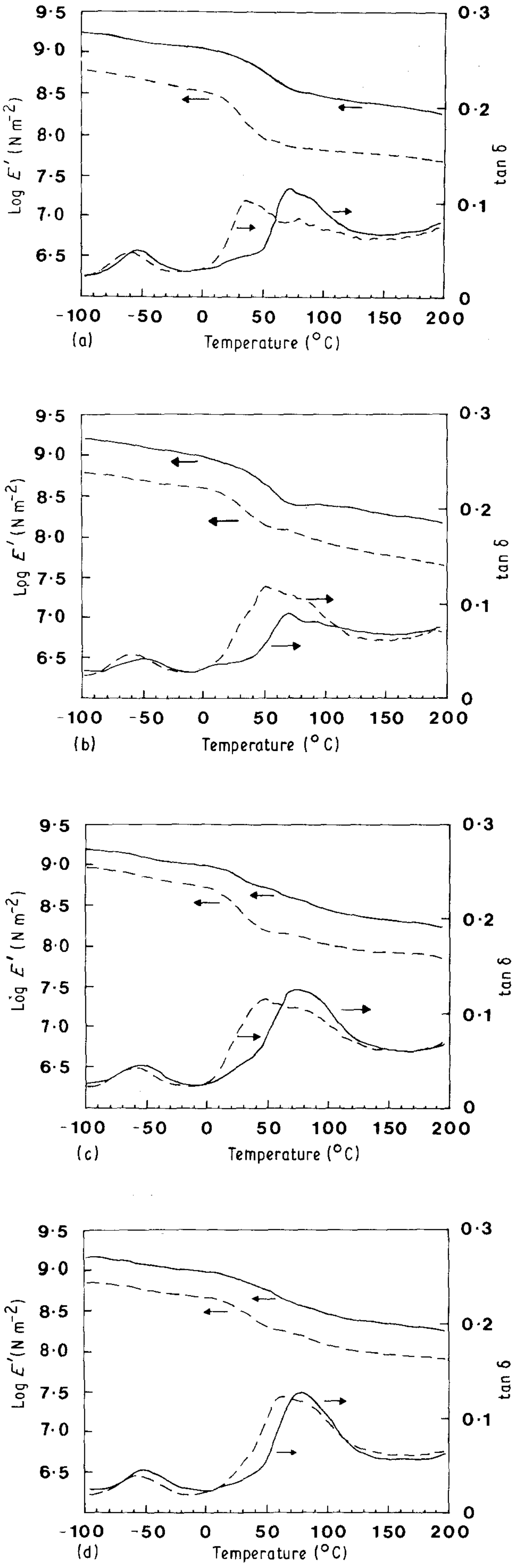

*Figure 3* DMTA traces for nylon 6,6 samples taken from different depths within injection-moulded bars. The solid lines correspond to a dry sample and the broken lines represent a conditioned bar. The depth ranges are (a) 0–0.2 mm; (b) 0.4–0.6 mm; (c) 1.0–1.2 mm; (d) 1.4–1.6 mm.

groups [6]. Storage of the bars in air allows water absorption (about 2% by weight) and the DMTA scans clearly show the plasticizing effect. Fig. 4 summarizes the values of $E'$ obtained at different depths and shows that on water absorption the modulus values typically exhibit almost a three-fold reduction. The tan δ peaks shift to lower temperatures and Fig. 5 shows that the effect of water absorption is greatest at the surface and reduces with depth from the surface. This correlates with the distribution of water within the bar since this is found to be highest at the surface. The glass transition temperature, taken to be indicated by the position of the tan δ peak, does not change much with depth in the dry bar (ca. 77 °C) but is very much lower at the surface in the conditioned state (ca. 36 °C) than near the centre (approaching 70 °C).

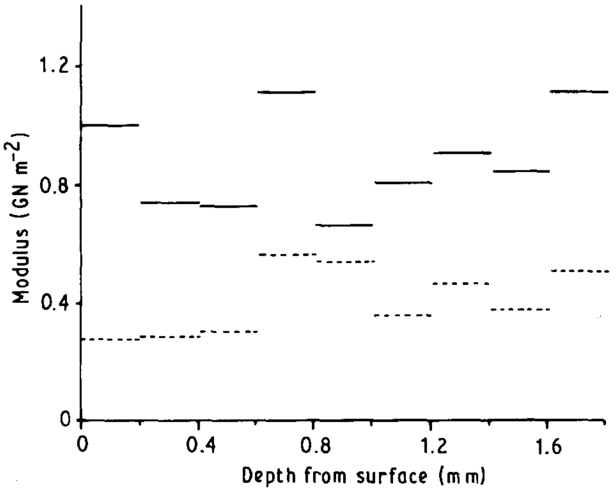

*Figure 4* Comparison of modulus values for dry (solid lines) and conditioned (broken lines) nylon 6,6 injection-moulded bars obtained by DMTA at room temperature.

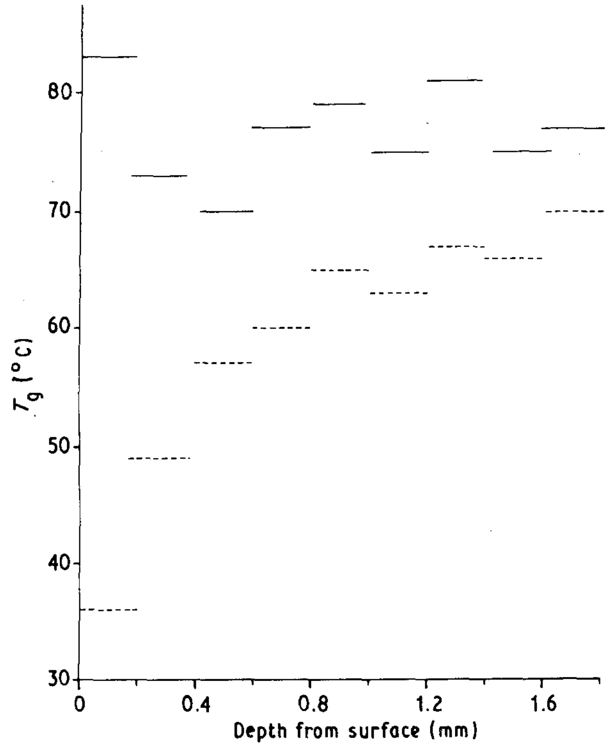

*Figure 5* Variation of $T_g$ (position of tan δ peak) with depth for dry (solid lines) and conditioned (broken lines) nylon 6,6 injection-moulded bars.

The $T_g$ for water-saturated nylon 6,6 samples extracted from bars immersed in water for 6 months is lower still, near 0 °C (Fig. 6). The drop in modulus in the water-saturated samples is more pronounced than that observed in dry bars or bars conditioned in laboratory air. The values at low temperature are generally slightly higher, an effect attributed to an antiplasticizing effect caused by the water molecules reducing the free volume and hindering chain movement [7, 10]. After $T_g$ there is an extensive region in which $E'$ remains unchanged or, in the case of the surface sample, increases slightly. This occurs at or just above 100 °C and is tentatively attributed to the loss of water, allowing hydrogen bonds to re-form in the nylon.

## 3.3. Through-depth modulus profiles

Injection mouldings produced from nylon 6,6 show large variations in Young's modulus as a function of depth. The plot of $S(a)$ versus $a$ for a dry A100S bar is shown in Fig. 7 with the resulting modulus profile displayed in Fig. 8. The modulus of the dry nylon bar is highest near the surface, then quickly falls to a minimum before increasing and levelling off towards the centre. O'Donnell [20] obtained similar results with polystyrene using the same technique, and Kamal and Moy [16, 17] found a similar profile for the sonic and tensile modulus distributions of semicrystalline polyethylene. The Young's modulus values for the skin in dry nylon 6,6 are about 1.2 times greater than for the core. The value for the ratio of Young's modulus in the skin and in the core, respectively, was found to be 1.6 in polypropylene by Fujiyama and Kimura [18]. The difference in the skin/core modulus values is attributed to the fact that the skin has a higher orientation than the spherulitic core. Many workers [16–19, 24] have found that maximum orientation occurs at or near the surface, with lower orientation found in the central regions.

A different profile was obtained for the water-saturated bars, as shown in Figs 9 and 10. The absolute Young's modulus values are significantly lower as

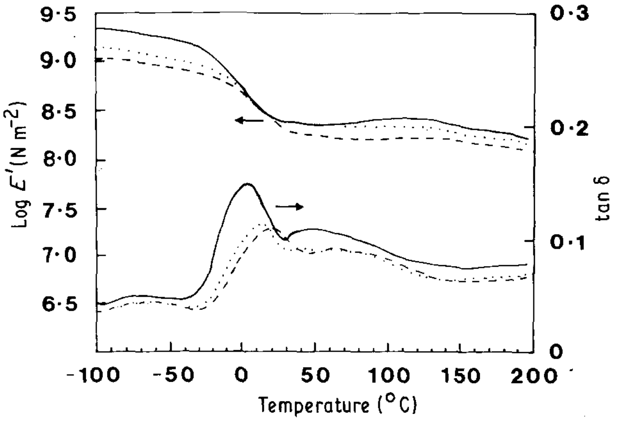

*Figure 6* DMTA traces for water-saturated nylon 6,6 samples taken from different depths of an injection-moulded bar. ———, 0–0.2 mm (skin); ....., 1.0–1.2 mm (intermediate); ----, 0.24 mm core material.

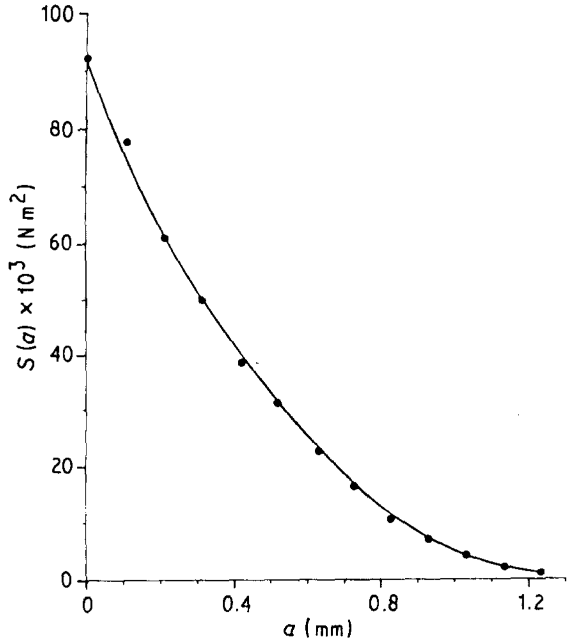

*Figure 7* Plot of $S(a)$ versus $a$, for a dry nylon 6,6 bar.

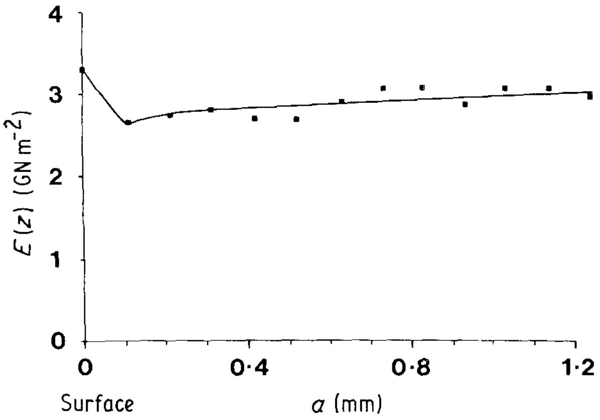

*Figure 8* Modulus profile for a dry nylon 6,6 injection-moulded bar obtained from Fig. 7.

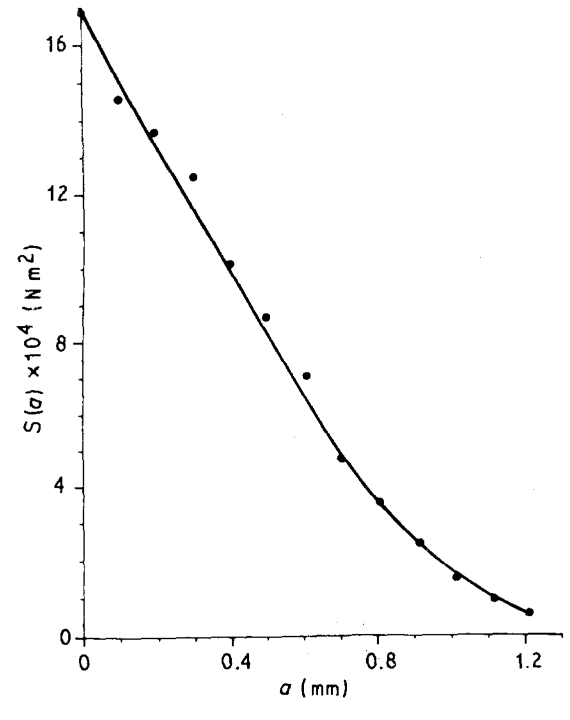

*Figure 9* Plot of $S(a)$ versus $a$, for a water-saturated nylon, 6,6 bar.

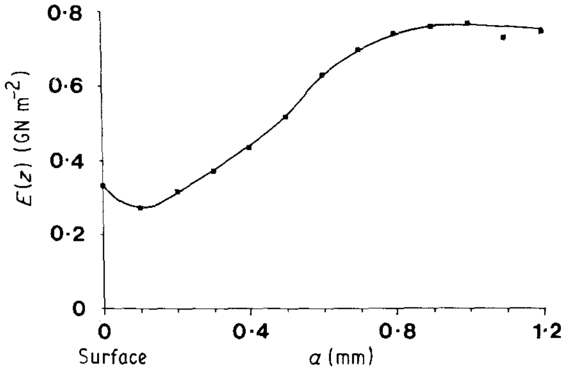

*Figure 10* Modulus profile for a water-saturated nylon 6,6 injection moulded bar obtained from Fig. 9.

a result of the plasticizing effect of water. The modulus at the surface is $\sim 0.35\,\mathrm{GN\,m^{-2}}$ then falls to $\sim 0.30\,\mathrm{GN\,m^{-2}}$ just in from the surface then rises to a constant value of $\sim 0.80\,\mathrm{GN\,m^{-2}}$ at a depth of 0.9 mm from the surface. The plasticizing effect of water is obviously greatest near the surface and least in the central regions. The magnitudes of both the wet and dry modulus profiles are in good agreement with the average values from the flexural test of $0.4\,\mathrm{GN\,m^{-2}}$ and $2.8\,\mathrm{GN\,m^{-2}}$, respectively.

The principal source of error in this technique for determining modulus variations arises from measuring the gradients from the graphs involved, particularly from the curved $S(a)$ versus $a$ plot. The gradients found near the ends of the $S(a)$ against $a$ graphs probably contain the largest errors; it is difficult to measure a gradient near the line extremities. This could have the effect of making the skin modulus values slightly too high. Another problem concerns the shape of the moulded bar; owing to thermal shrinkage the bar section is not perfectly rectangular but contains shallow sinking. The errors caused by this effect will be small and virtually disappear after the first milling operation, which makes the bar surface planar. Neither of the above problems affect the modulus profiles seriously except perhaps at the bar surface.

As mentioned earlier, this technique cannot determine the modulus values in the central $\sim 0.8$ mm core. This is not too much of a drawback with unfilled polymers for it is reasonable to assume that the constant value obtained as the centre is approached should continue right through the central core. This is because the thermal gradients and shear stresses are least in the central core and the morphology is uniform in a region that extends well beyond the 0.8 mm that is not covered in the above analysis.

### 3.4. Residual stress

Curvature profiles and residual stress distributions for a bar conditioned in laboratory air and a dry bar are shown in Figs 11 and 12. As expected, the stress distribution for a dry bar is quasi-parabolic, with compressive stresses in the surface areas and weaker tensile stresses in the inner regions. The maximum compressive stress is located at the surface, rising to

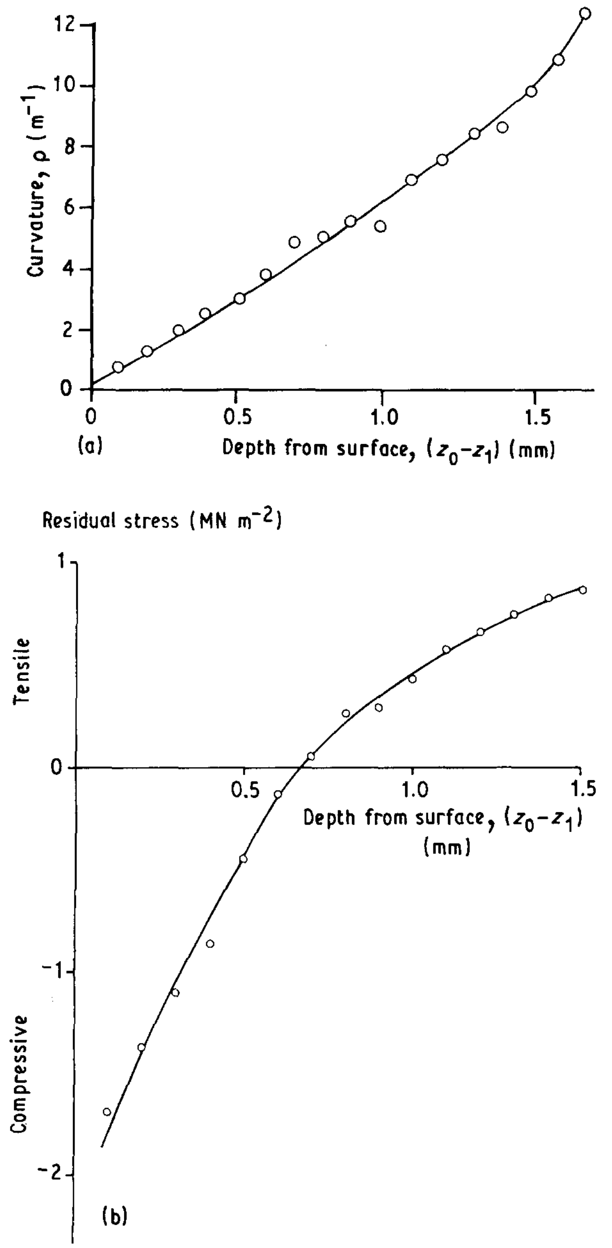

*Figure 11* Residual stress analysis for a conditioned nylon 6,6 bar. (a) Curvature profile; (b) residual stress distribution calculated using $E = 1.68\ \mathrm{GN\,m^{-2}}$.

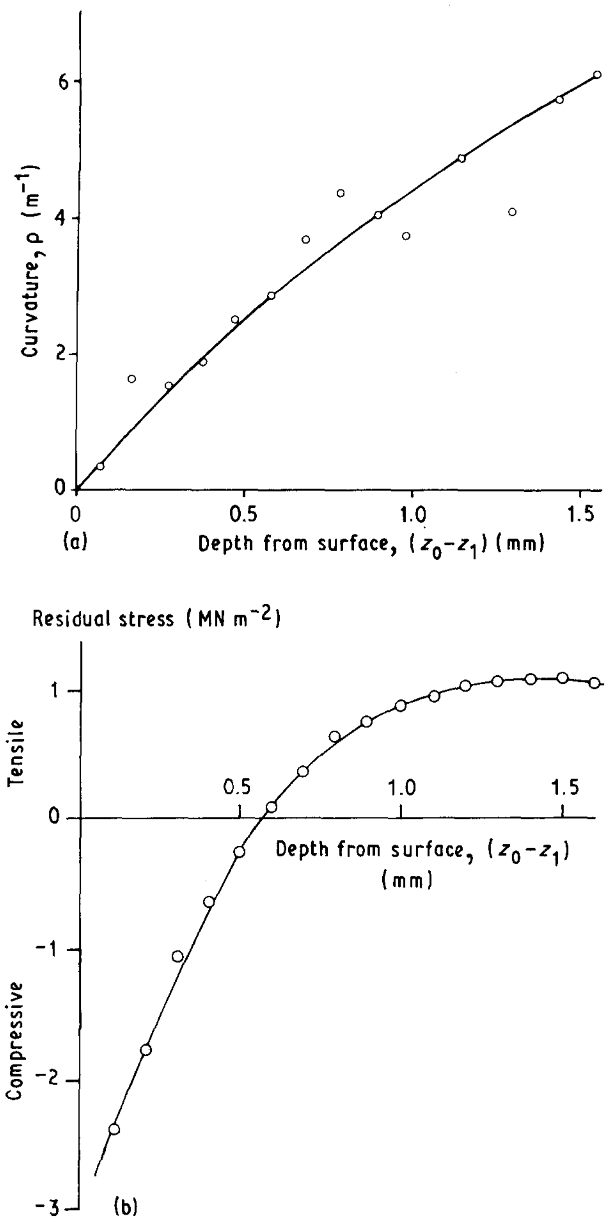

*Figure 12* Residual stress analysis for a dry nylon 6,6 bar. (a) Curvature profile; (b) residual stress distribution calculated using $E = 2.68\ \mathrm{GN\,m^{-2}}$.

ca. $3\ \mathrm{MN\,m^{-2}}$ while the maximum tensile stress is at the centre, with a value of about $1\ \mathrm{MN\,m^{-2}}$. Storage in air at room temperature allows the bars to pick up moisture and to undergo physical ageing. The as-moulded residual stress levels are reduced but the stress distribution remains quasi-parabolic. After long periods of time the residual stresses diminish to negligible values. They never completely relax in a semi-crystalline polymer such as nylon 6,6, probably due to the pinning effect of the crystalline regions, which prevent non-crystallized molecule segments from reaching a completely relaxed state. The relaxation of the residual stresses in polymers occurs with the residual stress field providing the driving force for its own relaxation [11]. This process will be helped by the presence of water inducing a plasticizing effect.

Water absorption causes a much greater change in the magnitude and distribution of residual stresses in nylons immersed long enough for water saturation to occur. On removing layers the curvature profile obtained is in the opposite sense to that found for dry bars as shown in Fig. 13a. This means that the residual stress distribution is likewise reversed, as shown in Fig. 13b, with strong tensile stresses in the surface regions and weaker compressive stresses in the interior. The water-saturated bars exhibit curvatures much greater than their dry counterparts. This does not mean that higher stresses are present, because water saturation causes a large reduction in modulus, making bending in response to imbalanced residual stresses much easier.

The presence of water also causes two more important changes that can have an effect on the residual stresses: secondary crystallization and swelling. Secondary crystallization is induced by the absorption of water [1, 12, 25]. When a moulding absorbs water the concentration in the outer regions is higher than in the interior and this leads to greater crystallization occurring near the surface. This is still observed to be

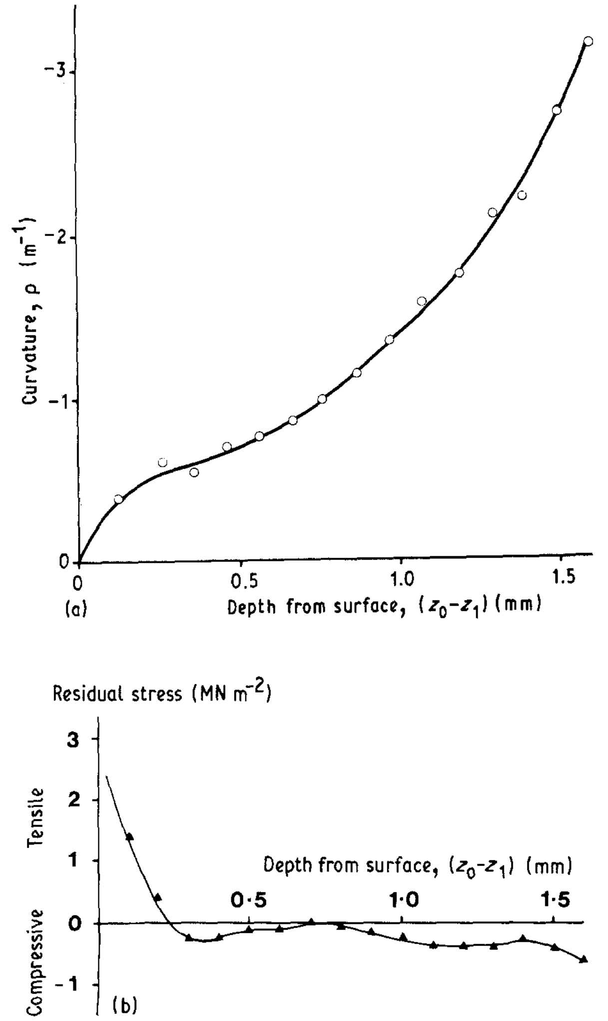

*Figure 13* (a) Curvature plot for a water-saturated nylon 6,6 bar ($E = 0.4\ \mathrm{GN\,m^{-2}}$). Note that the sense of curvature was opposite to that for the bars for which data are given in Figs 11a and 12a, and is assigned as negative; (b) residual stress profile for a water-saturated bar calculated from Fig. 13a showing tensile stresses near to the surface.

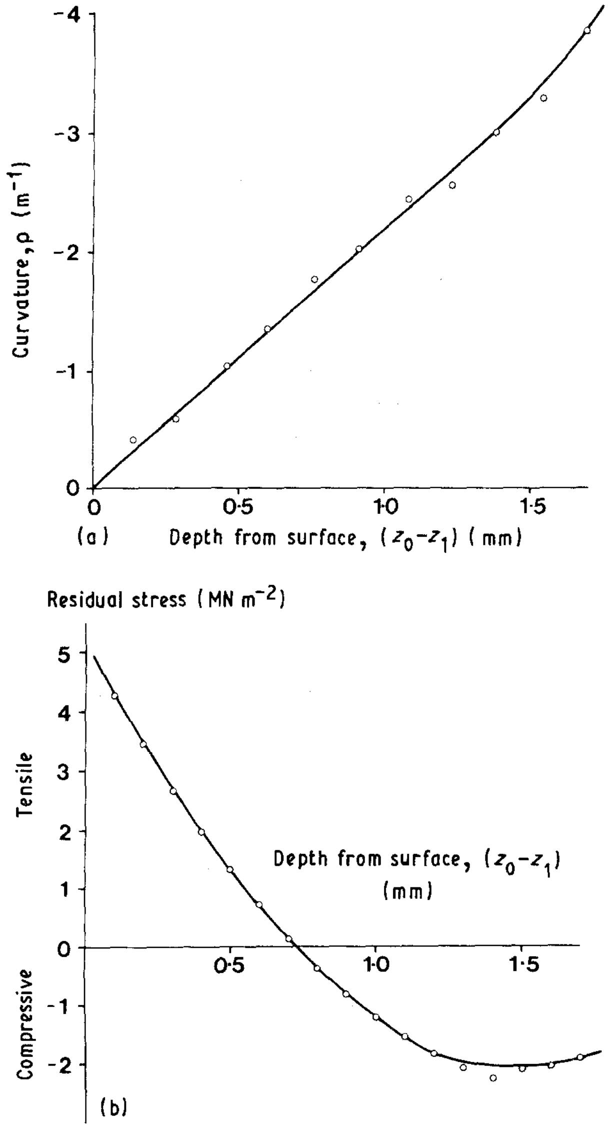

*Figure 14* (a) Curvature plot for a nylon 6,6 bar stored in water after moulding until saturation and then removed to laboratory air for 2 months before testing; (b) residual stress profile calculated using $E = 1.1\ \mathrm{GN\,m^{-2}}$.

true after very long times and we speculate that this may be the consequence of greater amounts of amorphous material in the skin as compared to that within the core, making the scope for secondary crystallization greatest in the skin. Transformation from amorphous to crystalline material produces a decrease in volume. This results in a greater volume reduction in the surface regions than in the central core because a greater fraction of material undergoes secondary crystallization near the surface. The initial effect of this is to reduce the moulded-in residual stress magnitude but with further secondary crystallization the residual stress distribution may reverse and with still further secondary crystallization the level of residual stresses will increase in this reversed sense.

The swelling caused by water absorption is unevenly distributed, with greater amounts in the outer regions. This should cause the as-moulded residual stresses to increase, that is, the greater swelling near the surface should cause a compressive increment there. Thus the change occurring as a consequence of swelling acts in the opposite sense to that due to secondary crystallization.

Fig. 14a shows a curvature profile for a nylon 6,6 bar sample which was water-saturated and then left to dry in air for several months. The water level reduced to 3.9% by weight and the overall Young's modulus measured in flexure increased to $1.1\ \mathrm{GN\,m^{-2}}$ from a value of $0.4\ \mathrm{GN\,m^{-2}}$. The curvature values are still significantly higher than for the dry or laboratory air conditioned samples, and the residual stress profile, Fig. 14b, shows tensile stresses in the surface areas and compressive stresses in the centre. That the stress distribution has not reverted to a state similar to that for bars simply conditioned in laboratory air is not too unexpected. The secondary crystallization produced during prolonged immersion in water is not reversible and the corresponding relative change in the volumes between the skin and core remains unaltered when desorption of water is allowed to occur.

## 3.5. Semi-quantitative assessment of the changes in residual stress levels

This section attempts to account for the observed changes in the residual stress distribution due to the three effects of water absorption: uneven swelling, Young's modulus reduction and secondary crystallization. The residual stress profiles for dry and water-saturated bars, labelled curve A and curve C respectively, are shown in Fig. 15 and the differences between them will now be examined.

### 3.5.1. *Swelling contribution*

The swelling caused by the uneven absorption of water makes stresses in the skin become more compressive and, conversely, the stresses in the core to become more tensile. From Fig. 2 the difference in water absorption between the skin and core is about 0.3% of the original volume. According to other workers [4, 10] a proportion of the water, estimated by them to be 20%, occupies what was formerly "free space" and if we suppose the actual volumetric change is 80% of the volume of water taken up, then the actual volume difference between the skin and core is $0.3 \times 0.8 = 0.24\%$. Assuming the volumetric expansion is isotropic, we can write that the relative linear expansion is 0.08%. If the fall in water content across the bar thickness is linear, then the change in stress due to this effect should be zero mid-way between the bar centre and surface. Measured from here, the maximum change in strain, which will occur at the surface and at the centre, is $0.5 \times 0.08 \times 10^{-2} = 4.0 \times 10^{-4}$. Therefore, at water saturation when the modulus is reduced to $400\,\mathrm{MN\,m^{-2}}$, this produces a maximum change in stress at the centre or surface of $400 \times 4.0 \times 10^{-4} = 0.16\,\mathrm{MN\,m^{-2}}$. Although this calculation is rather crude and is based on inexact assumptions and data, it does give a useful order of magnitude estimate for the size of the effect.

### 3.5.2. *Effect of the change in modulus*

To compare the two stress plots, A and C, we must first allow for the change in the magnitude of the stresses caused by the fall in modulus. Consider the effect of a uniform change in modulus on the residual stress distribution in a bar that is initially dry, then is immersed in water for a prolonged period. The relative strains through the depth of the bar remain unchanged if the modulus changes from one uniform value to another. Therefore the stress levels should change in proportion with the Young's modulus, and in the present sample should be reduced by 0.4/2.7. The result is plotted as dashed line B in Fig. 15. The measured distribution in water-saturated bars is plotted as curve C. The difference in stress levels between curves B and C at the centre is $0.65\,\mathrm{MN\,m^{-2}}$ and we now examine whether this can be explained by the swelling effect. Adding the contribution to swelling calculated in the previous section would cause the stresses shown in the intermediate curve, B, to increase, giving curve D. On comparing the experimental curve C and predicted curve D they are seen to be very different; they are found to be of opposite sense. The difference between A and C cannot therefore be explained by the swelling effect alone so attention is now focused onto the changes brought about by the secondary crystallization.

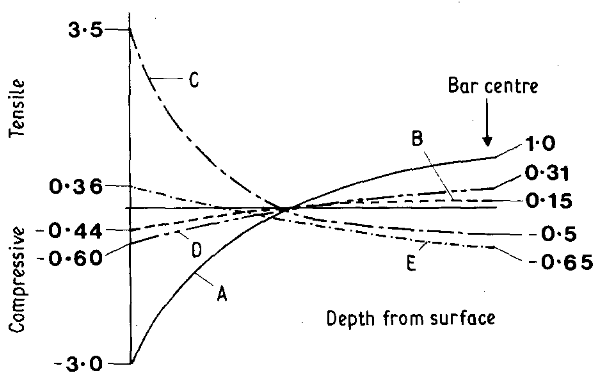

*Figure 15* Residual stress plots of dry and water-saturated nylon 6,6 bars and the combined effects of secondary crystallization and swelling. Curve A is the residual stress plot of a dry nylon 6,6 moulding. Curve B is the residual stress profile after allowing for the reduction in modulus induced by water absorption. Curve C is the stress profile for a water-saturated bar. Curve D is the residual stress curve after allowing for the water swelling effect. Curve E is the stress profile incorporating the secondary crystallization contribution.

### 3.5.3. *Effect of secondary crystallization*

Secondary crystallization acts in the opposite sense to the swelling, causing a tensile increment in the skin and a compressive increment in the core. The surface regions of a moulding are initially less crystalline as a result of rapid cooling during moulding whereas the interior cools more slowly and crystallizes more completely. The outer regions are then more prone to secondary crystallization. Taking crystallinity measurements from the literature [12, 25] and assuming that the crystallinity changes linearly through the depth we can construct Fig. 16. The relative volume changes at the surface and at the centre can be calculated using

$$\frac{V^{\mathrm{D}}}{V^{\mathrm{W}}} = \frac{\rho_{\mathrm{a}}^{\mathrm{W}} f_{\mathrm{a}}^{\mathrm{W}} + \rho_{\mathrm{cr}}^{\mathrm{W}} f_{\mathrm{cr}}^{\mathrm{W}}}{\rho_{\mathrm{a}}^{\mathrm{D}} f_{\mathrm{a}}^{\mathrm{D}} + \rho_{\mathrm{cr}}^{\mathrm{D}} f_{\mathrm{cr}}^{\mathrm{D}}} \tag{4}$$

where $V$ is specific volume, $\rho_{\mathrm{a}}$ is the density of amorphous polymer $= 1090\,\mathrm{kg\,m^{-3}}$, $\rho_{\mathrm{cr}}$ is the density of crystalline polymer $= 1240\,\mathrm{kg\,m^{-3}}$, $f_{\mathrm{a}}$ is the amorphous fraction, $f_{\mathrm{cr}}$ is the crystalline fraction $= 1 - f_{\mathrm{a}}$, and superscripts D and W indicate the dry

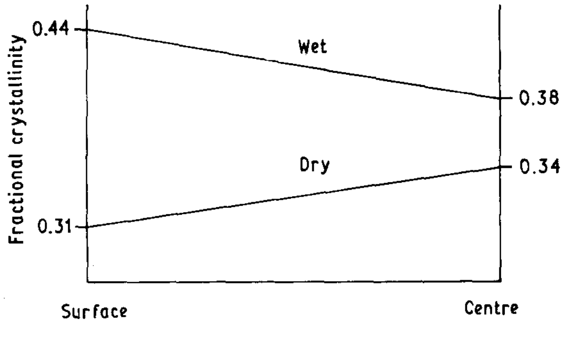

*Figure 16* Crystallinity changes as a consequence of water absorption in nylon 6,6.

and water-saturated state, respectively. Therefore using Equation 4, at water saturation the skin decreases in volume by 1.72% and the centre decreases in volume by 0.53%. The overall effect is that the skin decreases in volume 1.2% relative to the core. A similar approach to the swelling model is now used to calculate the effect on the stresses. If the volumetric contraction is isotropic, then the relative linear contraction is 0.4%. If the crystallinity changes are linear through the depth the change in stress midway between the centre and surface will be zero; therefore, measured from here, the maximum change in strain is 0.2%. If the modulus is $0.4\,\mathrm{GN\,m^{-2}}$, this causes a maximum change in stress at the surface or at the centre of $0.8\,\mathrm{MN\,m^{-2}}$ due to secondary crystallization. If we now return to Fig. 15, then using the procedure adopted before, the secondary crystallization would modify curve B to curve E. On comparing the predicted curve E and experimental curve C it is now found that the stress at the centre is compressive for both and that the magnitudes are very close. Thus it appears that secondary crystallization is the principal cause of the stress reversal in a water-saturated bar.

When the effects of secondary crystallization and swelling are superimposed the predicted stress level at the centre is $-0.49\,\mathrm{MN\,m^{-2}}$ $(0.15 - 0.8 + 0.16)$ which is in excellent agreement with the measured value of $-0.5\,\mathrm{MN\,m^{-2}}$.

In conclusion, it appears that at high water concentrations the secondary crystallization causes a relative volume change leading to the reversal of the residual stress distribution. This is opposed by a much smaller effect caused by the uneven swelling of the material. A similar approach to predict residual stress changes for bars containing low water levels (bars conditioned in air) shows that the uneven swelling effect is the dominant factor, with only small amounts of secondary crystallization taking place (only 1% difference between skin and core).

## 4. Conclusions

1. Injection mouldings of nylon 6,6 exhibit significant variations in properties through depth. The dry bars have a fairly uniform modulus over most of the interior but have a much higher modulus near the surface. Bars immersed in water until saturation show a large variation in modulus, with the plasticizing effect of water greatest near the surface. The relaxation temperatures fall with increasing water content and a bar containing a varying water concentration displays different $T_g$ values at different depths.

2. Nylon 6,6 mouldings with a modest water content (corresponding to absorption from laboratory air) have a quasi-parabolic residual stress distribution with compressive stresses in the surface regions and tensile stresses in the interior. The bars that were specially stored in a dry environment had greater residual stress levels than the bars that were conditioned in laboratory air and contained about 2% water.

3. The sense of the residual stresses reversed after prolonged immersion in water. At equilibrium the bars absorbed up to 9% water and this is believed to have induced secondary crystallization which was not uniform through the depth of the moulding and caused a relative volume change between the skin and core. This effect does not reverse on subsequent drying.

4. Three main influences of water on the residual stress distribution have been identified: (i) swelling, (ii) secondary crystallization and (iii) modification to the Young's modulus distribution. When water is taken up symmetrically the swelling causes the surface stresses to become more compressive and the stresses in the interior to become more tensile. The other factors act in the opposite direction.

5. Simple models have been developed to predict the effects of secondary crystallization and swelling on the residual stresses when water is absorbed symmetrically. The predicted changes in residual stress levels are in fair agreement with the experimental results.

## Acknowledgements

The authors would like to thank Dr D. R. Moore and his colleagues from ICI Wilton for useful discussions and the supply of the materials. MWAP is grateful to SERC for their financial support.

## References

1. M. I. KOHAN, (ed.) "Nylon Plastics" (Wiley-Interscience, New York, 1973).
2. W. E. NELSON, "Nylon Plastics Technology" (Newnes–Butterworths, London, 1976).
3. M. W. A. PATERSON, PhD Thesis, University of Newcastle upon Tyne, Newcastle upon Tyne (1990).
4. L. P. RAZUMOVSKII, V. S. MARKIN and G. YE. ZAIKOV, *Vysokomol Soyed.* **A27** (1985) 675. (English Translation: *Polymer Sci. USSR* **A27** (1985) 751.)
5. H. W. STARKWEATHER Jnr, *J. Macromol Sci. Phys. Ed.* **B3** (1969) 727.
6. N. G. McCRUM, B. E. READ and G. WILLIAMS, "Anelastic and Dielectric Effects in Polymeric Materials" (Wiley, London, 1967).
7. C. BIRKINSHAW, C. BUGGY and S. DALY, *Polym. Commun.* **28** (1987) 286.
8. A. E. WOODWARD, J. M. CRISSMAN and J. A. SAUER, *J. Polym. Sci.* **44** (1960) 23.
9. Maranyl Nylon, ICI Technical Data Sheet, NTD54 (1985).
10. H. W. STARKWEATHER Jnr, in "Water in Polymers", edited by S. P. Rowland (American Chemical Society, Washington DC, 1980) p. 433.
11. J. R. WHITE, *Polym. Test.* **4** (1984) 165.
12. D. P. RUSSELL and P. W. R. BEAUMONT, *J. Mater. Sci.* **15** (1980) 208.
13. Maranyl Nylon, ICI Technical Note, N102 (1973).
14. B. HAWORTH, G. J. SANDILANDS and J. R. WHITE, *Plast. Rub. Int.* **5** (1980) 109.
15. D. VALENTIN, F. PARAY and B. GUETTA, *J. Mater. Sci.* **22** (1987) 46.
16. M. R. KAMAL and F. H. MOY, *Polym. Eng. Rev.* **2** (1983) 381.
17. *Idem., Chem. Eng. Commun.* **12** (1981) 253.
18. M. FUJIYAMA and S. KIMURA, *Kobunshi Ronbunshu* **32** (1975) 591. (English translation: **4** (1975) 777).

19. P. G. LAFLEUR and M. R. KAMAL, *Polym. Eng. Sci.* **26** (1986) 103.
20. B. C. P. O'DONNELL, PhD thesis, University of Newcastle upon Tyne, Newcastle upon Tyne, (1990).
21. R. G. TREUTING and W. T. READ Jnr, *J. Appl. Phys.* **22** (1951) 130.
22. M. W. A. PATERSON and J. R. WHITE, *J. Mater. Sci.* **24** (1989) 3521.
23. B. L. DEOPURA, A. K. SENGUPTA and A. VERMA, *Polym. Commun.* **24** (1983) 287.
24. E. S. CLARK and G. A. GARBER, *Int. J. Polym. Mater.* **1** (1971) 31.
25. H. W. STARKWEATHER Jnr, G. E. MOORE, J. E. HANSEN, T. M. RODER and R. E. BROOKS, *J. Polym. Sci.* **21** (1956) 189.

*Received 18 November*
*and accepted 27 November 1991*